



**EVALUATION OF THE DRUG DELIVERY POTENTIAL OF CHITOSAN
NANOPARTICLES CARRYING DOXORUBICIN AND QUERCETIN USING
MOLECULAR MODELLING**

Chaitra K.¹, Durai Ananda Kumar T.², Subba Rao V. Madhupantula^{#3} and Asha Srinivasan^{#*1}

¹Division of Nanoscience and Technology, Faculty of Life Sciences, JSS Academy of Higher Education & Research, Mysore-570015, India.

²Department of Pharmaceutical Chemistry, JSS College of Pharmacy, JSS Academy of Higher Education & Research, Mysore-570015, India.

³Department of Biochemistry (DST-FIST Supported Department), JSS Medical College, JSS Academy of Higher Education & Research, Mysore-570015, India.

[#]Centre of Excellence in Molecular Biology and Regenerative Medicine (CEMR) Laboratory (DST-FIST Supported Centre), JSS Medical College, JSS Academy of Higher Education & Research, Mysore-570015, India.

***Corresponding Author: Dr. Asha Srinivasan**

Division of Nanoscience and Technology, Faculty of Life Sciences, JSS Academy of Higher Education & Research, Mysore-570015, India.

Article Received on 25/06/2020

Article Revised on 15/06/2020

Article Accepted on 06/07/2020

ABSTRACT

Chitosan nanoparticles offers a versatile biocompatible drug delivery system for several drugs. The interaction of nanoparticles with the drug molecules and the energy involved in the stabilization decides the efficiency of drug delivery systems. Molecular dynamic simulations provide the conformational stability analysis for the nanoparticles-drug complex. In our study the interaction between the chitosan nanoparticles and the drugs doxorubicin and quercetin is studied. The atomic level conformational stability between chitosan nanoparticles and drugs was demonstrated by the hydrogen bonds and π - π stacking interactions. The polar score for doxorubicin (2.2347 kcal/mol) with chitosan nanoparticles, doxorubicin with quercetin loaded chitosan nanoparticles (2.12 kcal/mol), quercetin with chitosan nanoparticles (1.27 kcal/mol) and quercetin with doxorubicin loaded chitosan nanoparticles (3.79 kcal/mol) is suggestive of spontaneous interactions and the complex is more stable. Molecular docking studies of doxorubicin and quercetin on the three-dimensional structures of P-gp (PDB-IDs: 6A6M and 6A6N) revealed the mechanism for the improved bioavailability of doxorubicin by quercetin. Quercetin established interaction with P-gp occurred through Mg^{2+} ion and Ser485, which is essential for the transport. Overall, the computational analysis suggests that chitosan nanoparticle as a potential nanocarrier for doxorubicin, and can be used for drug delivery systems.

KEYWORDS: Chitosan nanoparticles, Doxorubicin, Quercetin, Molecular dynamics simulation, P-glycoprotein.

INTRODUCTION

Doxorubicin (DOX) is an efficient anticancer drug, that inhibits the topoisomerase-II (TOP-II) and nucleic acid synthesis.^[1] DOX is used as first line therapy for breast cancer and lung cancer.^[2] Despite its excellent anti-tumor activity, the clinical efficacy of DOX is limited due to non-specificity, epithelial mesenchymal transition (EMT) and over expression of transforming growth factor- β (TGF- β).^[3] EMT is responsible for over expression of efflux ABC transporters, which promotes multidrug resistance (MDR) and decreases the bioavailability of the chemotherapeutic drugs.^[4] The co-administration of anticancer drugs with P-gp inhibitors namely Que and myricetin is an effective strategy for MDR reversal.^[5] The combination therapy is proven to be effective in achieving enhanced therapeutic benefit and overcoming the acquired drug resistance.^[6,7]

Quercetin (Que) is a plant flavonoid with anti-tumor activity that selectively inhibits the tyrosine kinase and down-regulates the efflux expression of ABC transporters (P-gp, BCRP and MRP1).^[8] DOX and Que combination therapy not only potentiates the anti-tumor effect of DOX but also attenuates its toxic effects.^[9] Our preliminary study indicated the ability of Que to decrease transforming growth factor- β (TGF- β) signaling in DOX treated breast cancer cells (MDA-MB-231 cells) by reducing the migratory potential.^[10] Several studies revealed the potential anticancer effect of combination of DOX and Que in human breast cancer cells. However, the small molecule Que activity is impaired by the associated poor pharmacokinetic characteristics.^[11]

Nanocarriers are used in delivering the combination of drugs, and this co-administration offers site

specificity.^[12] Concurrent release of two drug(s) from nanocarrier holds potential advantage of simultaneous intracellular drug delivery and with increased drug efficiency, while reducing collateral tissue toxicity. Several reports indicated the site specific delivery and controlled release of drugs using nanocarriers. Drug encapsulated nanoparticles reduces the cellular efflux process through enhanced permeation and retention (EPR effect) and augments the bioavailability of encapsulated drugs.^[13] DOX-nanoparticles produced anticancer activity even against the DOX resistant cancer cells along with the anti-MDR property.^[14] Quercetin-silica nanoparticles loaded DOX improved the bioavailability and improved intestinal permeation in more effective manner.^[15] Liposomal DOX formulations (Doxil[®], Lipodox[®]) are approved by FDA for the cancer clinical management. However, the interpatient pharmacokinetic variability and lack of stability is the major limitation of liposomal DOX.^[16-17] Also, the long term liposomal DOX therapy lowered the therapeutic efficacy compared with DOX monotherapy.^[18] This demands the more effective alternative nanocarrier. Chitosan is a natural cationic polymer and has controlled drug release and efflux pump inhibitory potential.^[19] Chitosan nanoparticles (CNPs) are known for biocompatibility, muco-adhesiveness and ability to open epithelial tight junctions.^[20] CNPs also offer pH dependent drug delivery and enhanced absorption of anticancer drugs.^[21]

Molecular dynamics simulations (MDS) help in understanding the molecular motions and ionic interactions between receptor (target) and drugs.^[22] The computational analysis provides basis for the development of nanoformulations.^[23] MDS assisted molecular interaction analysis evolved as an efficient strategy for the nanoformulation design.^[24] Yadav *et al.*, reported the encapsulation efficiency of chitosan for curcumin through molecular docking simulation study.^[25] Peng Shan *et al.*, investigated the molecular interactions between DOX and chitosan oligosaccharides (COS), and described the π - π interactions between the DOX and COS for the stability.^[26] Deepa *et al.*, reported the drug loading efficiency of chitosan nanoparticles for cytarabine through molecular dynamics simulations (MDS).^[27] Khezri *et al.*, demonstrated the chitosan incorporated curcumin as a biocompatible drug delivery form for the enhanced bioavailability through *in silico* analysis.^[28]

To the best of our knowledge there is no research work published on the DOX loaded Que-CNPs. In light of above mentioned facts, the present study aims at determining the molecular interactions of DOX and Que, in chitosan nanoparticle using *in silico* simulation studies. In the present investigation, the molecular interactions between the DOX and Que-CNPs as well as Que and DOX-CNPs revealed the structural stability and binding interaction energy of drug-nanocarrier complexes.

METHODS

Computational details

The two dimensional (2D) structures of DOX (PubChem CID: 31703), Que (PubChem CID: 5280343) and chitosan nanoparticle (PubChem CID: 71853) were downloaded from PubChem^[29] and converted into three-dimensional (3D) structures using OpenBabel^[30]. SYBYL X2.1.1 (Tripos international, St. Louis, MO), Discovery studio visualizer^[31], PRODRG server^[32], GROMACS 4.5.4^[33] and XMGRACE-5.1.22 program^[34] were utilized in the Molecular docking and simulations (MDS) studies.

Molecular dynamics simulation

The MDS for the drugs DOX and or QUE conjugated with CNPs was performed to predict their molecular affinity and stability. Initially, a molecular docking study on the CNPs (target) with drugs (DOX and or Que) was performed on SYBYL X 2.1.1. The docked poses with higher energy values were subjected for the MDS studies. The stability of the molecular docking poses of DOX-CNPs, Que-CNPs, Dox-CNPs-Que and Que-CNPs-Dox was investigated in GROMACS 4.5.4 using CHARMM27 force field. The binding free energy of start to end frames (i.e. ~1000 frames) of MD trajectories was determined by adopting Molecular Mechanics-Poisson-Boltzmann/Generalized Born Surface Area (MM-PBSA/MM-GBSA) method. The trajectory frames saved for every 1000 steps were subjected for cluster analysis using XMGRACE-5.1.22. The bonded (electrostatic) and non-bonded (van der Waal's) interactions were considered in the energy calculations. The supramolecular approach was applied for the calculation of total interaction energy (equation 1).^[35]

$$\Delta G_{\text{Bind}} = G_{\text{comp}} - (G_{\text{drug}} + G_{\text{carrier}}) \dots \dots \text{Equation 1}$$

In the equation, ΔG_{Bind} refers to interaction energy, G_{comp} stands for potential energy of drug-carrier complex, G_{drug} and G_{carrier} indicates the energies of drug and carrier, respectively. The atomic coordinates were placed in the octahedron box of ITP3P waters and neutralized by adding counter ions (9 chloride ions). Linear constraint solver (LINCS) algorithm and Steepest-Descent algorithm were utilized in the geometry optimization with a maximum of 5000 steps and a tolerance of 1000 kJ.mol⁻¹ nm⁻¹. Position restraints were applied and equilibrated by performing simulations using canonical ensembles (NVT) at a temperature of 300 K followed by isothermal-isobaric ensembles (NPT). Modified Berendsen thermostat and Parrinello-Rahman barostat methods were used to stabilize the temperature (300 K) and pressure (1.05 bar), respectively.

Molecular docking with P-gp

In order to understand the role of Que in overcoming the MDR (anti-MDR) and mechanism by which it improves the DOX bioavailability, we studied the influence of Que on the P-gp transporter protein through molecular docking studies. The three-dimensional (3D) structures of P-gp (PDB-IDs: 6A6M and 6A6N) was retrieved from protein

data bank (www.rcsb.org).^[36] The target protein was subjected to energy minimization after removing the water molecules and addition of charges on the SYBYL X 2.1.1 environment using Gasteiger-Marsiliand MMFF94s in convergence criterion of 0.05 kcal/mol. The active pocket of the target was determined through Protomol generation tool. The simultaneous docking of two ligands to the receptor binding pocket is not available in the literature and we attempted following the existing procedure with customization. Initially the docking of one ligand (Que/DOX) with the protein was performed, later the second ligand is docked (re-docking) to the previously docked protein complex in GEOMX mode. Four drug-protein complexes with two target proteins (Que-6A6M, Qu-6A6N, DOX-6A6M and DOX-6A6N) were generated and utilized in the re-docking.

RESULTS

Molecular docking and simulations analysis

The binding affinities of the drugs with the CNPs are investigated in the present study using MDS studies to understand the interaction details between the molecules, diffusion potential and complex stability of molecular components in the aqueous phase.^[37] In the SYBYL 2.1.1 X employed docking studies, the hydrogen bonding interactions between the drugs and CNPs produced stable complex. The energy profile provides the insights on van der Waal's and electrostatic interaction between drugs and CNPs. DOX established three hydrogen bonding interactions (polar score = 2.235 kcal/mol) with CNPs and five hydrogen bonding interactions with Que-CNPs (polar score = 4.07 Kcal/mol). Que established three hydrogen bonding with CNPs (polar score = 3.17 kcal/mol) and five hydrogen bonding with DOX_CNP (polar score = 4.52 Kcal/mol) (Figure 1, Table 1). The significant number of hydrogen bond interactions and higher polar interaction score (4.07 and 4.52 kcal/mol) indicates the stability of dual drug loaded CNPs (Table 1).

MDS trajectories were analyzed to reveal the interaction stability. The initial velocities were generated according to Maxwell distribution and the temperature coupling was performed using velocity rescaling with a coupling constant of 0.1 ps. Temperature-pressure coupling was performed using extended-ensemble Parrinello-Rahman algorithm with a coupling constant of 2 ps. The equilibrated system was then subjected for the MDS runs of 10 ns with a time step integration of 2 fs. The predominantly hydrophilic CNP did not interacted with either of the DOX and Que throughout the simulation. DOX and Que formed strong π - π stacking and hydrogen bond interactions, until the end of the simulation time. The binding free energy for the stabilization of DOX-CNPs with Que (-4.071 Kcal.mol⁻¹) is more acceptable. The cluster analysis also confirmed the mutual interactions. The binding free energy calculations estimated the total average (ΔG_{bind}) value for CNP and DOX complex (-51.31 Kcal/mol). The negative free energy (ΔG_{bind}) value of hydrogen bond contacts,

Coulomb energy, lipophilic packing and van der Waals interactions is suggestive of spontaneous interactions (Table 2, Figure 2). Gsolv accounts for linearized Poisson Boltzmann equation for each state (Polar) and the non-polar hydrophobic contribution of the system was calculated by the solvent accessible surface area. Entropic contribution was not considered in the analysis with an assumption that the binding of similar compounds with the chitosan nanoparticle will have nearly similar entropic contribution, which can be ignored in the calculations.^[38]

The molecular interactions between CNPs and drugs during the course of MDS was studied through various geometrical features such as heavy atoms RMSD, distance, Radius of gyration (Rg) and number of hydrogen bonds (Figure. 3). The overall interaction potential between chitosan nanoparticles and doxorubicin has been observed from the RDF plot (Figure 4). The RDF plot indicates that chitosan nanoparticles get closer to the doxorubicin drug molecule as observed from the first sharp peaks which located at about <2.0. Later on RDF falls and passes through a minimum value at ~4Å, which may be due to the strong repulsive forces between two molecules. However, at long distances, $g(r)$ versus r , represents the closest distance between the two atoms in the simulated system.

Molecular docking with P-gp

P-glycoprotein (P-gp, ABCB1, MDR1) is a unidirectional pump, which mediates the inward and outward transport of hydrophobic molecules.^[39] It is composed of two trans-membrane domains (TMDs) and two nucleotide-binding domain (NBDs). The binding of ATP to NBD is essential as it supplies energy for the transport. In an attempt to visualize the impact of Que on the transport, molecular docking of the transport proteins (6A6M and 6A6N) was carried out. The complexes of Que-6A6M, Que-6A6N, DOX- 6A6M and DOX-6A6N were utilized in the re-docking for the second ligand. The change of docking pose (conformation) of one ligand induced by the presence of second ligand was studied through simultaneous docking. The binding poses of individual ligands in presence of primary ligands were assessed complementary to its docking scores (Figure 5). In the docking study between Que and DOX_6A6M complex (predocked and saved), the bonding interaction between the Que and P-gp occurred through Mg²⁺ ion and Ser485, which extends the interaction with ATP (Fig 4). Magnesium (Mg²⁺) co-ordination with Ser485 and Gln529 controls the transport function.^[40] But in case of docking study between DOX and Que_6A6M complex, there is no H-bonding interaction between the Ser485 and Gln529. This can be considered as the reason for the enhanced bioavailability of DOX in presence of Que. In the docking study between Que and DOX_6A6N complex (predocked and saved), there is no H-bond interaction with Ser485, but the docking study of DOX with Que_6A6N revealed the possible hydrogen bond

interaction between the DOX and transporter. This also supports and confirms the previous hypothesis.

CONCLUSIONS

The atomic level conformational stability between chitosan nanoparticles and drugs was demonstrated by the hydrogen bonds and π - π stacking interactions. Overall, the computational analysis suggests that chitosan nanoparticle as a potential nanocarrier for doxorubicin, and can be used for dual drug delivery systems. Molecular docking studies of DOX and Que on

the three-dimensional (structures of P-gp (PDB-IDs: 6A6M and 6A6N) revealed the mechanism for the improved bioavailability of DOX by Que.

ACKNOWLEDGEMENTS

Dr. Asha Srinivasan thanks JSS Academy of Higher Education & Research for providing startup seed money. Mrs. Chaitra, K. thanks JSS Academy of Higher Education & Research for the award of JSS University Research Fellowship.

CONFLICT OF INTEREST

The authors declare that they have No Conflict of Interest reported in this paper.

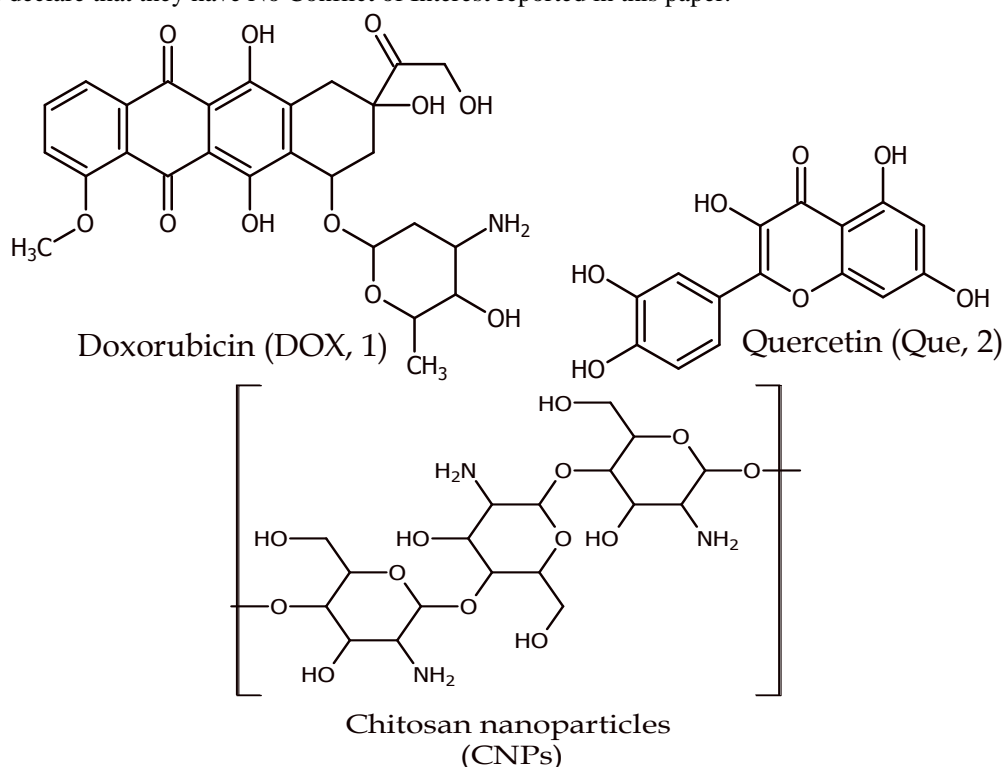


Table 1: Docking score and H-bond contact details of molecular docking.

Polymer	Drug	Score			H-Bond (Å)
		Total	Crash	Polar	
CNP	DOX	2.456	-1.058	2.298	CNP_CH ₂ OH – DOX_C ₁₄ -OH (1.98) CNP_NH ₂ – DOX_C ₇ -O-C ₁ * (2.05) CNP_CH ₂ OH – DOX_C ₉ -OH (2.22)
CNP	Que	2.304	-0.409	3.170	CNP_NH ₂ – Que_C ₃ *-OH (2.1) CNP_OH – Que_C ₃ -OH (1.91) CNP_CH ₂ OH – Que_C ₄ *-OH (1.94)
CNP_QUE	DOX	2.126	-1.034	4.071	Que-C ₅ -OH – O (DOX sugar) – (2.36) Que-CNP_CH ₂ OH – DOX-C ₁₄ -OH – (1.90) Que-CNP_NH ₂ – DOX-C ₉ -OH – (2.25) Que-CNP_OH – DOX-C ₆ -OH – (1.93) Que-CNP_OH – DOX-C ₅ =O – (2.22)
CNP_DOX	Que	3.790	-1.333	4.520	DOX-C ₉ -OH – Que-O ₁ – (2.13) DOX-C ₁₁ -OH – Que-C ₆ -OH – (1.88) DOX-CNP_CH ₂ OH – Que-C ₅ -OH – (1.96) DOX-CNP_NH ₂ – Que-C ₇ -OH – (2.08) DOX-CNP_O – Que-C ₇ -OH – (1.84)

CNP= Chitosan nanoparticles; DOX: Doxorubicin; Que= Quercetin

Table 2: MM-GBSA based binding free energy components.

Energy components (average)	Binding free energy (Kcal/mol)		
	CNPs and DOX	CNPs and Que	CNPs with DOX-Que complex
ΔG_{bind} Coulomb	-9.96	-14.78	-107.03
ΔG_{bind} Covalent	1.74	1.42	2.28
ΔG_{bind} H-bond	-0.92	-0.84	-1.77
ΔG_{bind} Lipo	-9.64	-8.38	-16.68
ΔG_{bind} Packing	-0.45	-0.43	-0.43
ΔG_{bind} Solv GB	15.41	21.49	125.02
ΔG_{bind} vdW	-26.33	-26.44	-52.70
Total - ΔG_{bind}	-30.15	-27.97	-51.31

ΔG_{Bind} = interaction energy; CNP= Chitosan nanoparticles; DOX: Doxorubicin; Que= Quercetin

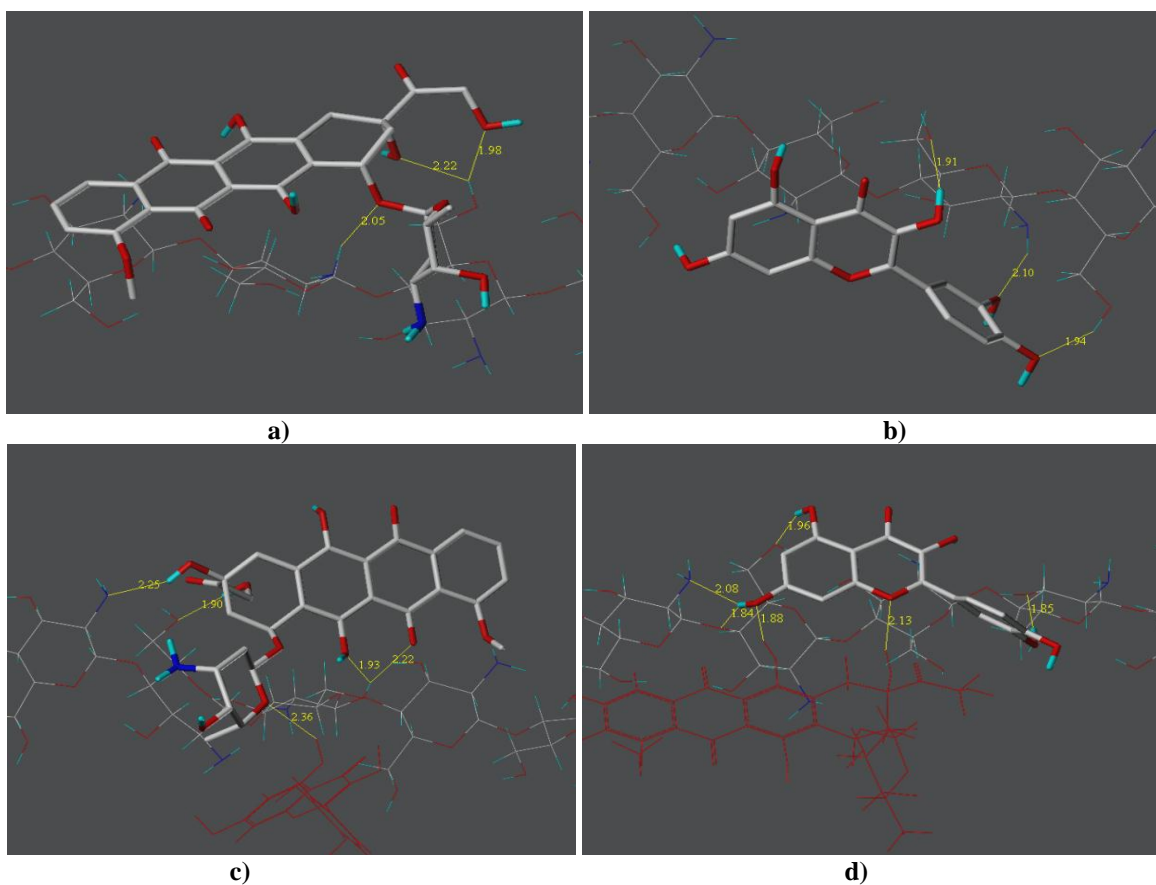


Figure 1: Three-dimensional (3D) molecular interaction visualization. a) CNPs and DOX, b) CNPs and Que, c) DOX to the Que-bound CNPs, d) Que to the DOX-bound CNPs.

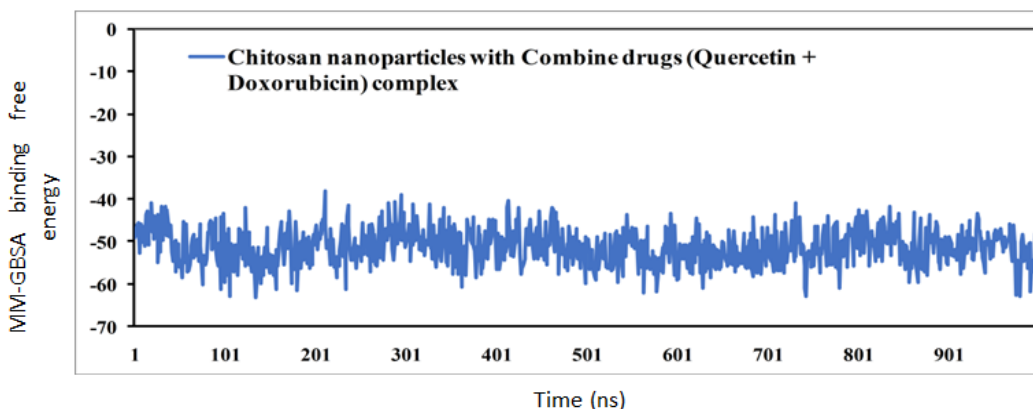


Figure 2: MM-GBSA energy profile of dual drug loaded chitosan nanoparticles.

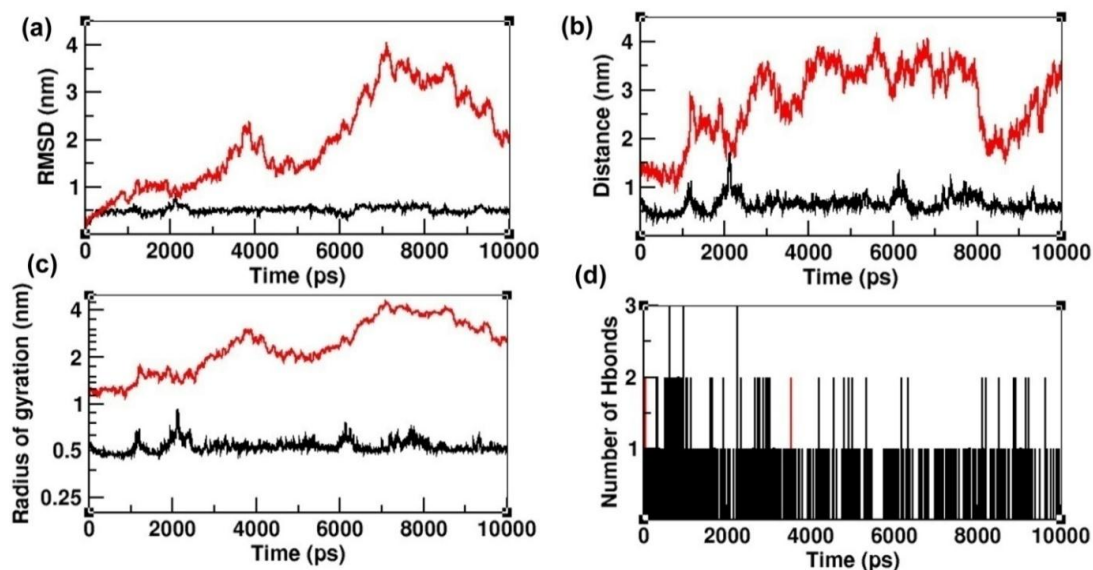


Figure 3: Analysis of geometrical features ((a) RMSD, (b) Distance, (c) Radius of gyrations, and (d) number of H-bonds) between quercetin and doxorubicin (represented in black trajectory lines) as well as quercetin doxorubicin drug complex and chitosan (represented in red trajectory lines).

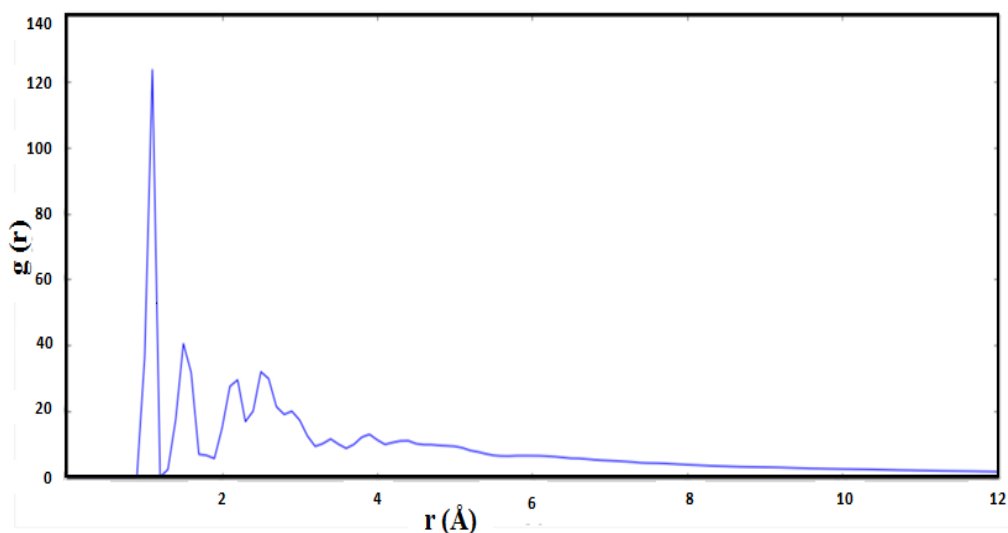
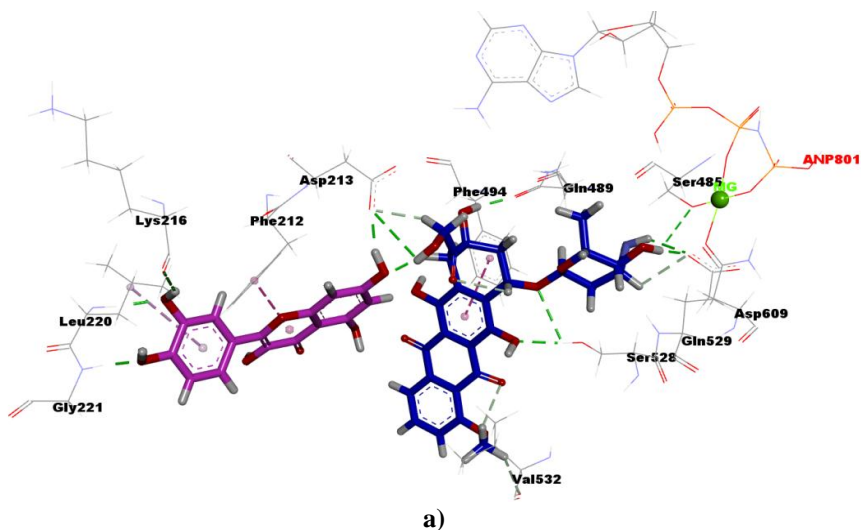
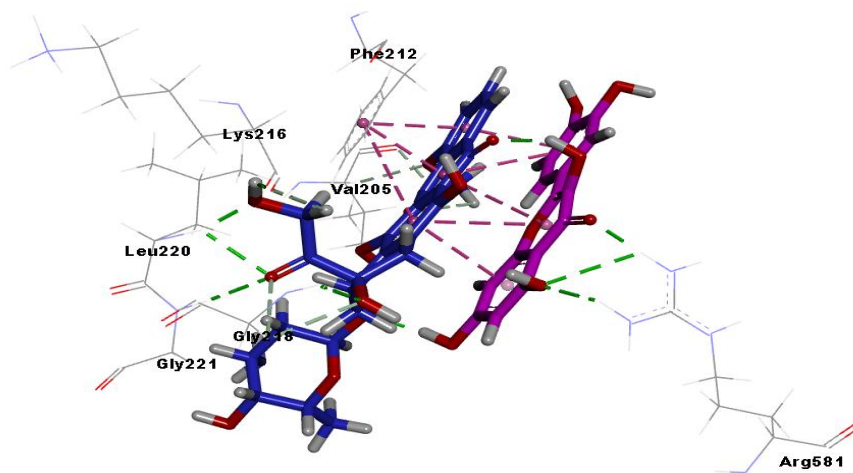
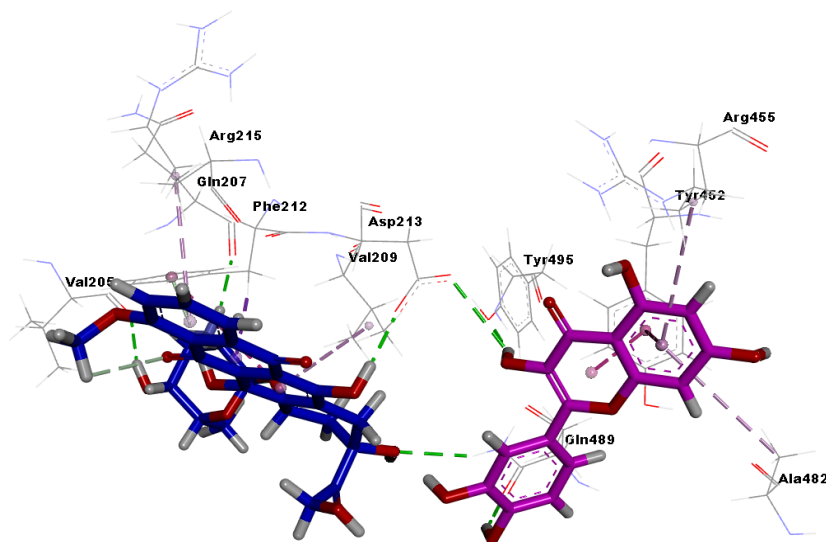


Figure 4: Radial distribution function (RDF) of chitosan nanoparticles and doxorubicin complex observed in MD simulation analysis.

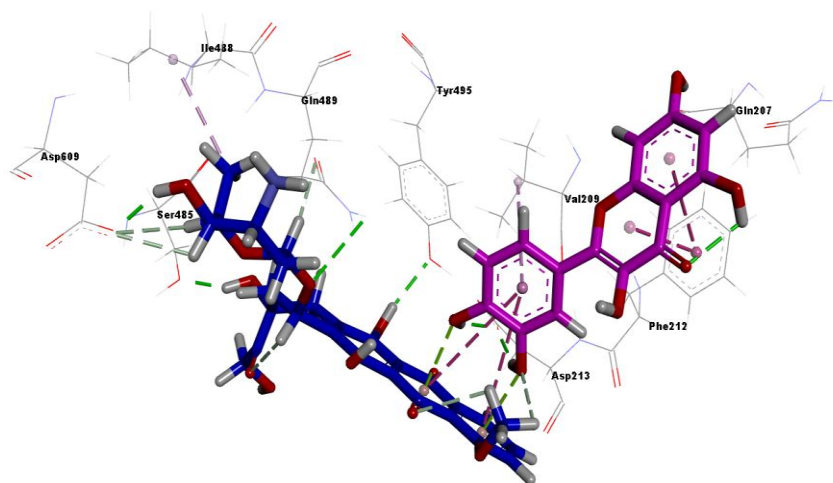




b)



c)



d)

Figure 5: Docking interactions poses. a) DOX to the Que_6A6M, b) Que to the DOX_6A6M, c) DOX to the Que_6A6N, d) Que to the DOX_6A6N

REFERENCES

1. N. Zhao, M. C Woodle, A.J. Mixson. *Advances in Delivery Systems for Doxorubicin*. J. Nanomed. Nanotechnol, 2018; 09: 519.
2. G. Zheng, M. Zheng, B. Yang, H. Fu, Y. Li. *Improving breast cancer therapy using doxorubicin loaded solid lipid nanoparticles: Synthesis of a novel arginine-glycine-aspartic tripeptide conjugated, pH sensitive lipid and evaluation of the nanomedicine in vitro and in vivo*. Biomed. Pharmacother, 2019; 116: 109006.
3. M. Cordani, R. Strippoli, Á. Somoza. *Nanomaterials as Inhibitors of Epithelial Mesenchymal Transition in Cancer Treatment*. *Cancers (Basel)*, 2019; 12: 25.
4. M. Gameiro, R. Silva, C. Rocha-Pereira, H. Carmo, F. Carvalho, M.D.L. Bastos, F. Remião. *Cellular models and in vitro assays for the screening of modulators of P-gp, MRP1 and BCRP*. *Molecules*, 2017; 22: 600.
5. S. Mohana, M. Ganesan, B. Agilan, R. Karthikeyan, G. Srithar, R. Beaulah Mary, D. Ananthakrishnan, D. Velmurugan, N. Rajendra Prasad, S. V Ambudkar. *Screening dietary flavonoids for the reversal of P-glycoprotein-mediated multidrug resistance in cancer*. *Mol. Biosyst*, 2016; 12: 2458–2470.
6. G. Du, H. Lin, M. Wang, S. Zhang, X. Wu, L. Lu, L. Ji, L. Yu. *Quercetin greatly improved therapeutic index of doxorubicin against 4T1 breast cancer by its opposing effects on HIF-1 α in tumor and normal cells*. *Cancer Chemother Pharmacol*, 2009; 65: 277–287.
7. S. Liu, R. Li, J. Qian, J. Sun, G. Li, J. Shen, Y. Xie. *Combination Therapy of Doxorubicin and Quercetin on Multidrug-Resistant Breast Cancer and Their Sequential Delivery by Reduction-Sensitive Hyaluronic Acid-Based Conjugate/d- α -Tocopheryl Poly(ethylene glycol) 1000 Succinate Mixed Micelles*. *Mol. Pharm*, 2020; 17: 1415–1427.
8. A.I. Alvarez, R. Real, M. Pérez, G. Mendoza, J.G. Prieto, G. Merino. *Modulation of the activity of ABC transporters (P-glycoprotein, MRP2, BCRP) by flavonoids and drug response*. *J. Pharm. Sci.*, 2010; 99: 598–617.
9. S. Li, S. Yuan, Q. Zhao, B. Wang, X. Wang, K. Li. *Quercetin enhances chemotherapeutic effect of doxorubicin against human breast cancer cells while reducing toxic side effects of it*. *Biomed. Pharmacother*, 2018; 100: 441–447.
10. A. Srinivasan, C. Thangavel, Y. Liu, S. Shoyele, R.B. Den, P. Selvakumar, A. Lakshmiikuttyamma. *Quercetin regulates β -catenin signaling and reduces the migration of triple negative breast cancer*. *Mol. Carcinog*, 2016; 55: 743–756.
11. D. Staedler, E. Idrizi, B.H. Kenzaoui, L. Juillerat-Jeanneret. *Drug combinations with quercetin: doxorubicin plus quercetin in human breast cancer cells*. *Cancer Chemother. Pharmacol*, 2011; 68: 1161–1172.
12. F.U. Din, W. Aman, I. Ullah, O.S. Qureshi, O. Mustapha, S. Shafique, A. Zeb. *Effective use of nanocarriers as drug delivery systems for the treatment of selected tumors*. *Int. J. Nanomedicine*, 2017; 12: 7291–7309.
13. E. Blanco, H. Shen, M. Ferrari. *Principles of nanoparticle design for overcoming biological barriers to drug delivery*. *Nat. Biotechnol*, 2015; 33: 941–951.
14. M. Zhang, E. Liu, Y. Cui, Y. Huang. *Nanotechnology-based combination therapy for overcoming multidrug-resistant cancer*. *Cancer Biol Med.*, 2017; 14: 212–227.
15. J. Fang, S. Zhang, X. Xue, X. Zhu, S. Song, B. Wang, L. Jiang, M. Qin, H. Liang, L. Gao. *Quercetin and doxorubicin co-delivery using mesoporous silica nanoparticles enhance the efficacy of gastric carcinoma chemotherapy*. *Int. J. Nanomedicine*, 2018; 13: 5113–5126.
16. A. Gabizon, R. Isacson, O. Rosengarten, D. Tzemach, H. Shmeeda, R. Sapir. *An open-label study to evaluate dose and cycle dependence of the pharmacokinetics of pegylated liposomal doxorubicin*. *Cancer Chemother. Pharmacol*, 2008; 61: 695–702.
17. R.F. Schell, B.J. Sidone, W.P. Caron, M.D. Walsh, T.F. White, B.A. Zamboni, R.K. Ramanathan, W.C. Zamboni. *Meta-analysis of inter-patient pharmacokinetic variability of liposomal and non-liposomal anticancer agents*. *Nanomedicine Nanotechnology. Biol. Med.*, 2014; 10: 109–117.
18. Y.L. Franco, T.R. Vaidya, S. Ait-Oudhia. *Anticancer and cardio-protective effects of liposomal doxorubicin in the treatment of breast cancer*. *Breast Cancer.*, 2018; 10: 131–141.
19. M.A. Mohammed, J.T.M. Syeda, K.M. Wasan, E.K. Wasan. *An Overview of Chitosan Nanoparticles and Its Application in Non-Parenteral Drug Delivery*. *Pharmaceutics*, 2017; 9: 53.
20. J. Ahmad, S. Akhter, N.H. Greig, M.A. Kamal, P. Midoux, C. Pichon. *Engineered Nanoparticles Against MDR in Cancer: The State of the Art and its Prospective*. *Curr. Pharm. Des.*, 2016; 22: 4360–4373.
21. A. Madhusudhan, G.B. Reddy, M. Venkatesham, G. Veerabhadram, D.A. Kumar, S. Natarajan, M.-Y. Yang, A. Hu, S.S. Singh. *Efficient pH dependent drug delivery to target cancer cells by gold nanoparticles capped with carboxymethyl chitosan*. *Int. J. Mol. Sci.*, 2014; 15: 8216–8234.
22. W.H.Z. Cárdenas, J.B. Mamani, T.T. Sibov, C.A. Caous, E. Amaro Jr, L.F. Gamarra. *Particokinetics: computational analysis of the superparamagnetic iron oxide nanoparticles deposition process*. *Int. J. Nanomedicine*, 2012; 7: 2699–2712.
23. A. Hospital, J.R. Goñi, M. Orozco, J.L. Gelpí. *Molecular dynamics simulations: advances and applications*. *Adv. Appl. Bioinform. Chem.*, 2015; 8: 37–47.
24. D. Essa, P.P.D. Kondiah, Y.E. Choonara, V. Pillay.

- The Design of Poly(lactide-co-glycolide) Nanocarriers for Medical Applications. *Front. Bioeng. Biotechnol.*, 2020; 8: 48.
25. P. Yadav, A. Bandyopadhyay, K. Sarkar, Enhancement of anticancer activity and drug delivery of chitosan-curcumin nanoparticle via molecular docking and simulation analysis, *Carbohydr. Polym.*, 2017; 182: 188-198.
 26. P. Shan, J.-W. Shen, D.-H. Xu, L.-Y. Shi, J. Gao, Y.-W. Lan, Q. Wang, X.-H. Wei. Molecular dynamics study on the interaction between doxorubicin and hydrophobically modified chitosan oligosaccharide. *RSC Adv*, 2014; 4: 23730–23739.
 27. G. Deepa, K.C. Sivakumar, T.P. Sajeewan. Molecular simulation and in vitro evaluation of chitosan nanoparticles as drug delivery systems for the controlled release of anticancer drug cytarabine against solid tumours. *3 Biotech*, 2018; 8: 493.
 28. A. Khezri, A. Karimi, F. Yazdian, M. Jokar, S.R. Mofradnia, H. Rashedi, Z. Tavakoli. Molecular dynamic of curcumin/chitosan interaction using a computational molecular approach: Emphasis on biofilm reduction. *Int. J. Biol. Macromol*, 2018; 114: 972–978.
 29. S. Kim, P.A. Thiessen, E.E. Bolton, J. Chen, G. Fu, A. Gindulyte, L. Han, J. He, S. He, B.A. Shoemaker, J. Wang, B. Yu, J. Zhang, S.H. Bryant. PubChem Substance and Compound databases. *Nucleic Acids Res.*, 2016; 44: D1202–D1213.
 30. N.M. O’Boyle, M. Banck, C.A. James, C. Morley, T. Vandermeersch, G.R. Hutchison. Open Babel: An open chemical toolbox. *J. Cheminform*, 2011; 3: 33.
 31. Dassault Systèmes BIOVIA, Discovery Studio Modeling Environment, Release 2017, San Diego: Dassault Systèmes, 2016.
 32. A.W. Schüttelkopf, D.M.F. van Aalten. PRODRG: a tool for high-throughput crystallography of proteinligand complexes. *Acta Crystallogr. Sect. D.*, 2004; 60: 1355–1363.
 33. H.J.C. Berendsen, D. van der Spoel, R. van Drunen. GROMACS: A message-passing parallel molecular dynamics implementation. *Comput. Phys. Commun*, 1995; 91: 43–56.
 34. Turner, P. J, XMGRACE, 5.1.19. Center For coastal and land-margin research, oregon graduate institute of science and technology, Beaverton, Ore, USA, 2005.
 35. S. Genheden, U. Ryde. The MM/PBSA and MM/GBSA methods to estimate ligand-binding affinities. *Expert Opin. Drug Discov*, 2015; 10: 449–461.
 36. H.M. Berman, J. Westbrook, Z. Feng, G. Gilliland, T.N. Bhat, H. Weissig, I.N. Shindyalov, P.E. Bourne. The Protein Data Bank, *Nucleic Acids Res.*, 2000; 28: 235–242.
 37. S. Sen, L. Nilsson, Structure, Interaction. Dynamics and Solvent Effects on the DNA-EcoRI complex in Aqueous Solution from Molecular Dynamics Simulation. *Biophys. J.*, 1999; 77: 1782–1800.
 38. N. Singh, A. Warshel. A comprehensive examination of the contributions to the binding entropy of protein-ligand complexes. *Proteins*, 2010; 78: 1724–1735.
 39. F.J. Sharom. Complex Interplay between the P-Glycoprotein Multidrug Efflux Pump and the Membrane: Its Role in Modulating Protein Function. *Front. Oncol*, 2014; 4: 41.
 40. A. Kodan, T. Yamaguchi, T. Nakatsu, K. Matsuoka, Y. Kimura, K. Ueda, H. Kato. Inward- and outward-facing X-ray crystal structures of homodimeric P-glycoprotein CmABCB1, *Nat. Commun*, 2019; 10: 88.